JOURNAL OF APPLIED ELECTROCHEMISTRY **19** (1989) 271–274

Studies of the kinetics of aluminium incorporation into an iron electrode in molten salts by linear sweep voltammetry

F. LANTELME, E. CHERRAT

Laboratoire d'Electrochimie, U.A. 430 CNRS, B'.F, Université Pierre et Marie Curie, 4 Place Jussieu, F75252 Paris Cedex 05, France

Y. CHRYSSOULAKIS, S. KALOGEROPOULOU

Laboratoire de Chimie-physique, Ecole Polytechnique d'Athènes, 9 rue Iroon Polytechniou, Zografou, Athenes, Greece

Received 12 May 1988; revised 25 July 1988

The deposition of aluminium on iron leads initially to the formation of a solid solution which may be useful to protect the iron substrate from oxidation. This incorporation can be carried out at high temperature by electrochemical reduction of aluminium ions in a fused electrolyte ($LiCl–KCl–AlCl_3$). In the present investigation linear sweep voltammetry is used to study the interdiffusion process which controls the metal incorporation. The results are interpreted within the framework of a theoretical treatment previously described. However it is shown that a more refined analysis is required to take into account the predominant role of the thermodynamic properties of the alloys and the influence of the movement of the electrode–electrolyte interface during the electrolysis.

1. Introduction

Aluminium is a prospective alloying element to protect iron from oxidation by forming a protective alumina film [1]. A significant amount of research has been devoted to the metal incorporation into a substrate by fused salt electrolysis [2]. The kinetics of growth of diffusion layers plays an important rôle in the determination of optimum operational parameters. The aim of the present paper is to show that the electrochemical techniques are convenient not only to prepare protective coatings but also to give fundamental information about the metal interdiffusion which controls the formation of the alloy layers.

Recently we presented a theoretical interpretation of cyclic voltammograms carried out on an alloy electrode [3]. This technique was used here to study aluminium incorporation into an iron matrix. Some experiments using the potential step technique will be also described.

2. Experimental details

The principle of the linear sweep voltammetry experiments is simple: the electroreduction of aluminium ions dissolved in a fused electrolyte was carried out on a working electrode which was a rod (diameter ca 1 mm) of pure iron (Johnson Matthey, 15 ppm total metallic impurities); then the alloyed aluminium was reoxidized. The potential variations were such that the alloy composition remained in the concentration range of the solid solution (α phase: $0 < X_{red} < 0.5$, X_{red} being the mole fraction of aluminium).

These processes were performed by use of a triangular potential sweep. The counter electrode and the reference electrode were rods of pure aluminium (Johnson Matthey, 20 ppm total metallic impurities). The potential and current variations were recorded on a digital oscilloscope (Nicolet 3091). The same device was used for the potential step experiments.

The electrolyte was a fused LiCl–KCl eutectic mixture. The aluminium ions were introduced to the bath at a concentration $C^*_{ox} \simeq 0.1 \text{ mol l}^{-1}$ by anodic oxidation of a plate of pure aluminium. For more experimental details see our previous description [4].

3. Linear sweep voltammetry

3.1. *Description of the voltammograms*

A typical voltammogram is represented in Fig. 1. It is characterized by a sharp maximum which occurs at the most negative potential, E_M, and by a bump appearing during the oxidation process. The potential of this maximum of the oxidation current is denoted E_m; E_i is the most positive potential.

3.2. *Interpretation*

As the diffusion coefficient, D_{ox}, of the aluminium ions is far greater than the metal interdiffusion coefficient, $\tilde{D}_{red}$, the change of the concentration, C_{ox}, at the electrode surface can be considered negligible. Under these conditions it has been shown [3] that when the potential window is large enough with respect to

0021-891X/89 $03.00 + .12 © 1989 Chapman and Hall Ltd.

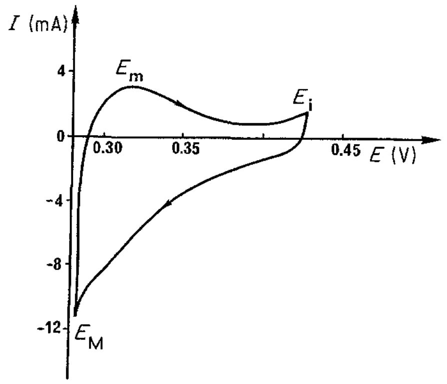

Fig. 1. Voltammogram for the reaction $Al^{3+} + 3e \rightarrow Al$ on an iron electrode ($S = 1.42\,cm^2$) in an LiCl–KCl eutectic mixture containing $AlCl_3$ ($C^*_{Al3+} = 0.286\,mole\,l^{-1}$). Temperature: 747 K. Potential window: $E_i = 0.425\,V$, $E_M = 0.278\,V$ vs Al/Al^{3+} electrode. Sweep rate: $\upsilon = 0.147\,V\,s^{-1}$.

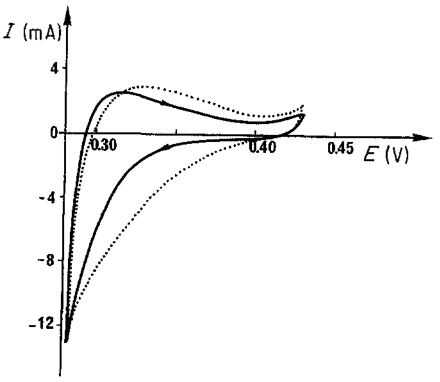

Fig. 2. Calculated voltammograms for the experimental values given in Fig. 1. Full line: theoretical voltammogram deduced from Equations 1 and 2. Dotted line: results of the numerical calculations taking into account the concentration dependence of the activity factor, f_{red}, and the movement of the electrode–electrolyte interface.

RT/nF the voltammogram obeys the equations

forward sweep

$$i = i_M \exp(-\xi) \tag{1}$$

backward sweep

$$i = i_M[\exp(\xi)\, erfc(\xi^{1/2}) - 2\pi^{-1/2} Daw(\xi^{1/2})] \tag{2}$$

erfc and *Daw* are respectively the complementary error function and the Dawson integral [5]. A similar equation has been used by Schiffrin [6] to describe the reversible electrodeposition of insoluble products; ξ is an adimensional parameter representing the potential $\xi = \mathscr{F}(E - E_m)$ with $\mathscr{F} = nF/RT$; i_M is the current density at E_M

$$i_M = -nF(C^*_{ox}/f_{red})(\tilde{D}_{red}\mathscr{F}v)^{1/2} \exp(\xi^0) \tag{3}$$

v is the potential sweep rate and ξ^0 is $\mathscr{F}(E^0 - E_M)$. The value E^0 of the standard potential of the redox couple is deduced from our previous experiments [7]. C^*_{ox} is the bulk concentration of the oxidized species. Equation 1 indicates that a maximum, i_m, of the oxidation current occurs at a potential, E_m [3]. These two values should obey the relations

$$i_m/i_M = -0.194 \tag{4}$$

$$\xi_m = \mathscr{F}(E_m - E_M) = 1.367 \tag{5}$$

The activity factor, f_{red} [8], of the reduced species (aluminium) is deduced from the thermodynamic properties of the aluminium–iron system [9]. Here a mean constant value is chosen which corresponds to the composition of the alloy in the region of the current maximum.

In order to obtain a potential window large enough to apply the preceding analysis the potential, E_i, has to reach values for which a slight oxidation of the iron substrate is observed. This contribution can be easily calculated from our previous experiments concerning the Fe/Fe^{2+} system [3].

The interdiffusion coefficient, $\tilde{D}_{red}$, is calculated by a least squares procedure in order to obtain the best fit of the curves deduced from Equations 1, 2 and 3 to the experimental curves. An example of theoretical and experimental curves is shown in Figs 1 and 2. The values of the interdiffusion coefficients deduced from the different experiments are reported in Table 1. In this table are also reported the values of the potential difference, $\xi_m = \mathscr{F}(E_m - E_M)$, and of the current ratio, i_m/i_M; most of these experimental values are greater than the theoretical values (Equations 4 and 5). This departure could be due to the approximations in the theoretical treatment. Indeed in establishing Equations 1 and 2, we assumed that the activity factor, f_{red}, remained constant in the experimental concentration range. Moreover the movement of the electrode–electrolyte interface due to the metal incorporation during the electrolysis was neglected. The influence of these two phenomena was examined following the procedure described hereafter. Under the moving boundary conditions the diffusion equation diffusion becomes

$$dC_{red}/dt = \tilde{D}_{red} d^2C_{red}/dx^2 - u\,dC_{red}/dx \tag{6}$$

where u is the velocity of the movement of the interface. The integration of this equation has already been carried out [10] only under galvanostatic or potentiostatic conditions. We use here the numerical integration technique [11]. The concentration, $C_{red}(0, t)$, at the electrode surface is given by Nernst's law

$$C_{red}(0, t) = \frac{C_{ox}}{f_{red}} \exp[-\mathscr{F}(E - E^0)] \tag{7}$$

The activity factor, f_{red}, is deduced from the thermodynamic data [9]; a polynomial expansion is used to express the dependence of the activity coefficient, γ_{red}, on the mole fraction, X_{red}, of the alloy

$$\ln \gamma_{red} = a_0 + a_1(1 - X_{red}) + a_2(1 - X_{red})^2 + a_3(1 - X_{red})^3 \tag{8}$$

The values of the coefficients a_i are: $a_0 = 21.545$, $a_1 = -94.196$, $a_2 = 102.62$, $a_3 = -41.495$. The activity factor, f_{red}, is linked to γ_{red} through the equation

$$f_{red} = \gamma_{red}[X_{red}M_{red} + (1 - X_{red})M_s]/\sigma \tag{9}$$

M_{red} and M_s are the atomic masses of the electroactive metal and of the substrate; σ is the specific mass of the

Table 1. Characteristic points of the experimental voltammograms: potential window E_i, E_M vs Al^{3+}/Al electrode ($C^*_{Al^{3+}} = 0.286\,mol\,l^{-1}$), potential difference, $\xi_m = nF(E_m - E_M)/RT$ and current ratio, i_m/i_M. v: sweep rate. X_M: Al at% at E_M. $\tilde{D}_{red}$: interdiffusion coefficient in the system Al-Fe (iron-rich side, α-phase) calculated from the theoretical representation (Equations 2 and 3). Temperature: 747 K

Exp. No.	Experimental values						$\tilde{D}_{red}$ ($10^{-12}\,cm^2\,s^{-1}$)
	v (Vs^{-1})	E_i (V)	E_m (V)	X_M (%)	ξ_m	$-i_m/i_M$	
1	0.244	0.425	0.303	4.3	0.886	0.266	1.7
2	0.289	0.425	0.280	8.1	1.147	0.449	1.2
3	0.147	0.425	0.278	8.6	1.406	0.340	0.62
4	2.117	0.482	0.270	10.3	2.143	0.651	1.1
5	0.448	0.491	0.267	11.1	1.886	0.500	0.48
6	0.226	0.491	0.265	11.6	1.710	0.364	0.32
7	0.383	0.425	0.233	20.7	3.392	0.786	0.23
8	0.195	0.425	0.230	21.9	3.014	0.617	0.13

alloy. The interdiffusion coefficient, $\tilde{D}_{red}$, is chosen in order to obtain the best representation of the experimental curves. An example of these results is shown in Fig. 2. The values of the interdiffusion coefficients, $\tilde{D}_{red}$, of the potential difference, $\xi_m = \mathcal{F}(E_m - E_M)$ and of the current ratio, i_m/i_M, are reported in Table 2. It is shown that taking into account the concentration dependence of the activity factor and the movement of the interface improves the representation of the voltammograms. The calculated current ratios are greater than the classical value (Equation 4), but these ratios remain smaller than the experimental results. This observation is linked to the shape of the experimental voltammograms which indicates that the current at the beginning of the reducing period is always greater than the theoretical and calculated currents (Figs 1 and 2). The shape of the oxidation part of the experimental voltammograms being similar to that obtain from Equation 2, this effect induces a greater value for the current maximum, i_m. As indicated in Table 2 a more detailed analysis reveals the predominant influence of the activity coefficient. This observation is in agreement with our previous conclusions [3] which indicated the high sensitivity of this analysis to the thermodynamic properties of the system, for example a change of ±3 mV of the standard potential, E^0, induces a variation of ±30% on $\tilde{D}_{red}$.

Table 2. Results of the numerical calculations taking into account the concentration dependence of the activity factor, f_{red}, and the influence of the movement of the electrode–electrolyte interface

Exp No.	ξ_m	$-i_m/i_M$	$\tilde{D}_{red}$ ($10^{-12}\,cm^2\,s^{-1}$)	$\tilde{D}$* ($10^{-12}\,cm^2\,s^{-1}$)
1	1.345	0.224	2.2	2.4
2	1.753	0.245	2.7	3.1
3	1.849	0.250	1.3	1.5
4	2.006	0.257	3.1	3.7
5	2.157	0.261	1.3	1.6
6	2.073	0.260	0.80	0.95
7	2.558	0.278	1.2	1.8
8	2.639	0.282	0.99	1.5

* Values obtained without taking into account the movement of the electrode–electrolyte interface.

Moreover as usual [10] the calculations performed without taking into account the movement of the interface overestimate the values of the diffusion coefficients. However this influence remains small with respect to the perturbations created by the variations of the activity coefficients.

4. Chronoamperometry

Two complementary experiments were carried out using the potential step technique. In order to obtain a current response not too small with respect to the current noise (≃ 0.1 mA) a sufficiently large potential jump was required; the concentration range was then greater than that examined during the voltammetry. The recorded chronoamperograms reported in Fig. 3 were exploited according to the Cottrell law

$$i = nF(C^*_{red} - C_{red})D^{1/2}_{red}(\pi t)^{-1/2} \qquad (10)$$

The bulk concentration, C^*_{red}, and the surface concentration, C_{red}, are calculated (Equation 7) from the values of the starting potential, E^*, and of the potential during the pulse, $E_p = E^* + \Delta E$, ΔE being the potential step. These calculations are performed taking into account the thermodynamic properties of the alloys as indicated by Equation 8. The crude results from Cottrell's law are corrected from the influence of the movement of the interface according to the procedure already described [10]. This correction becomes important when the aluminium concentration increases. The results (Fig. 2) are of the same order of magnitude as those deduced from the linear sweep voltammetry. As already pointed out [12] it seems that in the studied concentration range the aluminium concentration does not influence the value of the interdiffusion coefficient very much.

5. Conclusion

Our results concerning the interdiffusion of aluminium and iron in the concentration range of the α solid solution are in agreement with the previous measurements of Fellner *et al.* [12]. These authors studied the interdiffusion in the system Fe–Al either by determining the distribution of aluminium by means of an

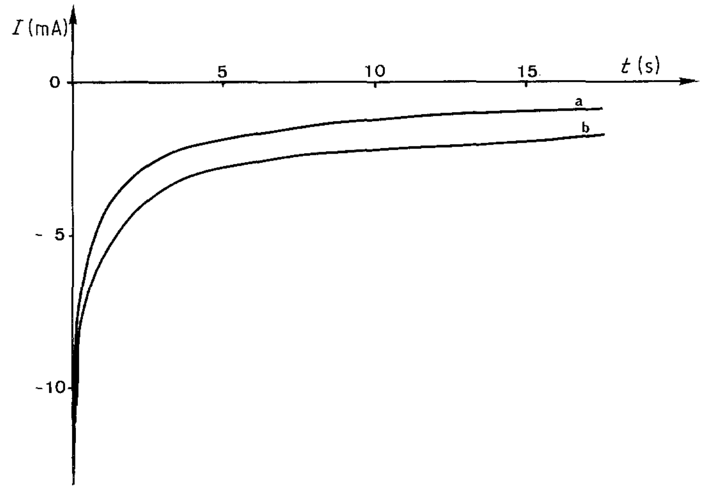

Fig. 3. Chronoamperogram for the reduction of aluminium ions in an LiCl–KCl eutectic mixture ($C^*_{Al3+} = 0.095\,\mathrm{mole\,l^{-1}}$) at 747 K. Curve a: $E^* = 0.452$ V vs Al^{3+}/Al electrode, $\eta = -0.35$ V, $X_{Al} = 42$ Al at%, calculated $\tilde{D}_{red} = 0.45 \times 10^{-12}\,\mathrm{cm^2\,s^{-1}}$. Curve b: $E^* = 0.5$ V vs Al^{3+}/Al electrode, $\eta = -0.35$ V, $X_{Al} = 30$ Al at%, $\tilde{D}_{red} = 1.3 \times 10^{-12}\,\mathrm{cm^2\,s^{-1}}$.

electron microprobe or by determining the thickness of the diffusion layer by anodic dissolution. The results given by these two techniques are in good agreement. For very thin layers the method of anodic dissolution was found to be more sensitive than the determination using the electron probe. At 757 K Fellner *et al.* [12] indicate $\tilde{D}_{red} = 5.4 \times 10^{-12}\,\mathrm{cm^2\,s^{-1}}$; our mean value is smaller: $\tilde{D}_{red} = 1.50 \times 10^{-12}\,\mathrm{cm^2\,s^{-1}}$. This difference remains in the range of accuracy of the experiments. Moreover this difference is relatively small when we consider the value $\tilde{D}_{red} \simeq 10^{-14}\,\mathrm{cm^2\,s^{-1}}$ (25 at% Al) at 747 K extrapolated from diffusion-penetration curves carried out in the temperature range 800–1100° C [13]. This departure probably reflects the influence of the contribution of the grain boundary diffusion which becomes important at low temperature.

The present study indicates that the transient electrochemical techniques provide a rapid and convenient means of studying the formation of alloy coating on a metallic electrode. This is all the more interesting as these coatings can also be built up by electrochemical deposition.

The much used linear sweep voltammetry technique may be used to obtain suitable information about the interdiffusion process which controls the formation of the alloy coating. The theoretical analysis previously given [3] provides a convenient interpretation of the experimental voltammograms; so the order of magnitude of the interdiffusion coefficient is rapidly obtained. However by using a more refined analysis it is shown in the present paper that important features of the metal interdiffusion have to be taken into account. This mainly concerns the thermodynamic properties of the alloys and the departure from ideality which occurs during the concentration changes inherent in the electrolytic process. To a less extent this detailed analysis indicates that the movement of the interface due to the dissolution or to the deposition of the electroactive metal should also be taken into account; neglecting this influence overestimates the values of the interdiffusion coefficients. These phenomena may be of some importance when the metal deposition under cyclic or pulsed potentials is considered.

Acknowledgement

The authors would like to thank the Commission of European Communities for the Development of Joint Study Programmes for a grant awarded to one of them (S.K.).

References

[1] H. A. Ahmed and W. W. Smeltzer, *J. Electrochem. Soc.* **133** (1986) 212.

[2] N. C. Cook, *Sci. Am.* **221** (1969) 38.

[3] F. Lantelme and E. Cherrat, *J. Electroanal. Chem.* **244** (1988) 61.

[4] F. Lantelme, D. Inman and D. G. Lovering, in 'Molten Salt Techniques' (edited by R. J. Gale and D. G. Lovering), Plenum Press, New York (1984) Vol. 2, p. 181.

[5] M. Abramowitz and I. A. Stegun, 'Handbook of Mathematical Functions', 9th edn, Dover Publications, New York (1972).

[6] D. J. Schiffrin, *J. Electroanal. Chem.* **201** (1986) 199.

[7] F. Lantelme, H. Alexopoulos, M. Chemla and O. Haas, *Electrochim. Acta* **33** (1988) 761.

[8] F. Lantelme, Y. Iwadate, Y. Shi and M. Chemla, *J. Electroanal. Chem.* **187** (1985) 229.

[9] J. Eldridge and K. L. Komarek, *Trans. AIME* **230** (1964) 226.

[10] F. Lantelme, *J. Electroanal. Chem.* **196** (1985) 227.

[11] A. J. Bard and L. R. Faulkner, 'Electrochemical Methods, Fundamentals and Applications', Wiley, New York (1980) p. 675.

[12] P. Fellner, M. Chrencová-Paucirová and K. Matiašovsky, *Surface Tech.* **8** (1979) 501.

[13] J. Hirvonen, *J. Appl. Phys.* **52** (1981) 6143.